A Cluster of Aromatic Residues in the Sixth Membrane-Spanning Segment of the Dopamine D2 Receptor Is Accessible in the Binding-Site Crevice[†]

Jonathan A. Javitch,*[,‡,§] Juan A. Ballesteros,[||] Harel Weinstein,[||] and Jiayun Chen[‡]

Center for Molecular Recognition and Departments of Psychiatry and Pharmacology, College of Physicians and Surgeons, Columbia University, 630 West 168th Street, New York, New York 10032, and Department of Physiology and Biophysics, Mount Sinai School of Medicine, New York, New York 10029

Received September 9, 1997; Revised Manuscript Received November 7, 1997[⊗]

ABSTRACT: The binding site of the dopamine D2 receptor, like that of other homologous G protein-coupled receptors, is contained within a water-accessible crevice formed among its seven membrane-spanning segments. Using the substituted-cysteine accessibility method, we previously mapped the residues in the third, fifth, and seventh membrane-spanning segments that contribute to the surface of this binding-site crevice. We have now mutated to cysteine, one at a time, 22 consecutive residues in the sixth membrane-spanning segment (M6) and expressed the mutant receptors in HEK 293 cells. Ten of these mutants reacted with charged, hydrophilic, lipophobic, sulfhydryl-specific reagents, added extracellularly, and all but one were protected from reaction by a reversible dopamine antagonist, sulpiride. Thus, we infer that the side chains of the residues at the reactive loci (V378, F382, W386, P388, F389, F390, T392, H393, I394, and I397) are on the water-accessible surface of the binding-site crevice. The pattern of accessibility is consistent with an α-helical conformation with a wide angle of accessibility near the binding site itself and a narrower stripe continuing toward the cytoplasmic portion of the binding-site crevice. This pattern of accessibility is consistent with the presence of a proline kink which could bend the extracellular portion of M6 into the binding-site crevice where it would be more broadly accessible than the cytoplasmic portion of the membrane-spanning segment. Four highly conserved aromatic residues and a histidine are clustered together on the water-accessible surface of the binding-site crevice. They define an interconnected "aromatic cluster" that may be involved in ligand binding and receptor activation.

The dopamine receptors, like the homologous receptors for the other biogenic amines, bind neurotransmitters present in the extracellular medium and couple this binding to the activation of intracellular G-proteins (*1*, *2*). The binding sites of these receptors are formed among their seven, mostly hydrophobic, membrane-spanning segments (*2*, *3*) and are accessible to charged, water-soluble agonists, like dopamine. Thus, for each of these receptors, the binding site is contained within a water-accessible crevice, the binding-site crevice, extending from the extracellular surface of the receptor into the transmembrane portion. The surface of this crevice is formed by residues that can contact specific agonists and/or antagonists and by other residues that may play a structural role and affect binding indirectly.

To identify the residues that form the surface of the binding-site crevice in the human D2 receptor, we have used the substituted-cysteine accessibility method (SCAM)[1] (*4*−*9*). Consecutive residues in the membrane-spanning segments are mutated to cysteine, one at a time, and the mutant receptors are expressed in heterologous cells. If ligand binding to a cysteine-substitution mutant is near-normal, we assume that the structure of the mutant receptor, especially around the binding site, is similar to that of the wild type and that the substituted cysteine lies in an orientation similar to that of the wild-type residue. In the membrane-spanning segments, the sulfhydryl of a cysteine facing into the binding-site crevice should react much faster with charged, polar, sulfhydryl-specific reagents than should sulfhydryls facing into the interior of the protein or into the lipid bilayer. For such reagents, we use derivatives of methanethiosulfonate (MTS): positively charged MTS ethylammonium ($MTSEA^+$) and MTS ethyltrimethylammonium ($MTSET^+$) and negatively charged MTS ethylsulfonate ($MTSES^-$) (*10*). These reagents are about the same size as dopamine, with maximum dimensions of approximately 10 Å by 6 Å. They form mixed disulfides with the cysteine sulfhydryl, covalently linking SCH_2CH_2X, where X is NH_3^+, $N(CH_3)_3^+$, or SO_3^-. We use two criteria for identifying an engineered cysteine as forming the surface of the binding-site crevice. (i) The reaction with

[†] This work was supported in part by NIH Grants MH01030 and MH54137, by the G. Harold & Leila Y. Mathers Charitable Trust, and by the Lebovitz Trust (J.A.J.) and by NIH Grants DA09083 and DA00060 (H.W.).

[‡] Center for Molecular Recognition, Columbia University.

[§] Departments of Psychiatry and Pharmacology, Columbia University.

[||] Mount Sinai School of Medicine.

[⊗] Abstract published in *Advance ACS Abstracts,* December 15, 1997.

[1] Abbreviations: SCAM, substituted-cysteine accessibility method; M3, third membrane-spanning segment; M5, fifth membrane-spanning segment; M6, sixth membrane-spanning segment; M7, seventh membrane-spanning segment; MTS, methanethiosulfonate; $MTSEA^+$, MTS ethylammonium; $MTSET^+$, MTS ethyltrimethylammonium; $MTSES^-$, MTS ethylsulfonate; MMTS, methylmethanethiosulfonate; GPCRs, G-protein-coupled receptors.

S0006-2960(97)02241-1 CCC: $15.00
Published on Web 01/13/1998

an MTS reagent alters binding irreversibly; (ii) this reaction is retarded by the presence of ligand.

On the basis of site-directed mutagenesis experiments, many laboratories have implicated residues in the sixth membrane-spanning segment (M6) of G-protein-coupled receptors (GPCRs) in binding and in receptor activation (*11*). Moreover, in rhodopsin, the β2 adrenergic receptor, and the $5HT2_A$ receptor, movement of M6 has been associated with receptor activation (*12*−*16*). Here, we report the application of SCAM in identifying systematically all the residues in M6 of the D2 receptor that contribute to the binding-site crevice.

EXPERIMENTAL PROCEDURES

Numbering of Residues. Residues are numbered according to their positions in the human dopamine $D2_L$ receptor sequence. In some cases, we also index residues relative to the most conserved residue in the membrane-spanning segment in which it is located (*17*). By definition, the most conserved residue is assigned the position index "50", e.g. Pro388$^{(6.50)}$, and therefore Leu387$^{(6.49)}$ and Phe389$^{(6.51)}$. This indexing simplifies the identification of corresponding residues in different GPCRs.

Site-Directed Mutagenesis. Cysteine mutations were generated as described previously (*7*). Mutations were confirmed by DNA sequencing. Mutants are named as (wild-type residue)(residue number)(mutant residue), where the residues are given in the single-letter code.

Construction of the Epitope-Tagged D2 Receptor Construct. The sequence encoding the β2 adrenergic receptor epitope-tagged at the amino terminus with the cleavable influenza-hemagglutinin signal sequence followed by the "FLAG" epitope (IBI, New Haven, CT) was a gift from B. Kobilka (*18*). The sequence encoding the epitope tag was excised and ligated in-frame to the D2 receptor cDNA, thereby creating a fusion protein in which the epitope tag led directly into the sequence of the D2 receptor. This epitope-tagged D2 receptor fragment was then subcloned into the bicistronic expression vector pcin4 (a gift from S. Rees, Glaxo) (*19*).

Transient and Stable Transfection. HEK 293 cells in DMEM/F12 (1:1) with 10% bovine calf serum (Hyclone) and 293-TSA cells (a clonal line of HEK 293 cells stably expressing the SV40 large T antigen) in DMEM with 10% fetal calf serum were maintained at 37 °C and in 5% CO_2. For transient transfection, 35 mm dishes of 293-TSA cells at 70−80% confluence were transfected with 2 μg of the wild type or mutant D2 receptor cDNA in pcDNA1/Amp (Invitrogen) or pcin4 (see above) using 9 μL of lipofectamine (Gibco) and 1 mL of OPTIMEM (Gibco). Five hours after transfection, the solution was removed and fresh medium added. Twenty-four hours after transfection, the medium was changed. Forty-eight hours after transfection, cells were harvested as described below. For stable transfection, HEK 293 cells were transfected with D2 receptor cDNA in pcin4 as described above. Twenty-four hours after transfection, the cells were split to a 100 mm dish and 700 μg/mL Geneticin was added to select for a stably transfected pool of cells. The affinity of the epitope-tagged receptor for *N*-methylspiperone, YM-09151-2, and sulpiride was unchanged from that of the wild-type receptor, and no differences in binding affinity or accessibility to the MTS reagents were detected between receptor from transiently and stably transfected HEK 293 cells.

Harvesting Cells. Cells were washed with phosphate-buffered saline (PBS; 8.1 mM NaH_2PO_4, 1.5 mM KH_2PO_4, 138 mM NaCl, and 2.7 mM KCl at pH 7.2), briefly treated with PBS containing 5 mM EDTA, and then dissociated in PBS. Cells were pelleted at 1000*g* for 5 min at 4 °C, and resuspended for binding or treatment with MTS reagents.

[^{3}H]-N-Methylspiperone Binding. Whole cells from a 35 mm plate were suspended in 400 μL of buffer A (25 mM HEPES, 140 mM NaCl, 5.4 mM KCl, 1 mM EDTA, and 0.006% BSA at pH 7.4). Cells were then diluted 20-fold with buffer A. [^{3}H]-*N*-Methylspiperone (Dupont/NEN) binding was performed as described previously (*9*). Depending on the level of expression in the various mutants, adjustments in the number of cells per assay tube were made as necessary to prevent depletion of ligand in the case of very high expression or to increase the signal in the case of low expression.

Reactions with MTS Reagents. Whole cells from a 35 mm plate were suspended in 400 μL of buffer A. Aliquots (50 μL) of cell suspension were incubated with freshly prepared MTS reagents at the stated concentrations at room temperature for 2 min. Cell suspensions were then diluted 20-fold, and 300 μL aliquots were used to assay for [^{3}H]-*N*-methylspiperone (200 pM) binding as described (*9*). The fractional inhibition was calculated as 1 − [(specific binding after the MTS reagent)/(specific binding without the reagent)]. We used the SPSS for Windows (SPSS, Inc.) statistical software to analyze the effects of the MTS reagents by one-way ANOVA according to Dunnett's post hoc test ($p < 0.05$).

The second-order rate constant (k) for the reaction of $MTSEA^+$ with each susceptible mutant was estimated by determining the extent of reaction after a fixed time, 2 min, with four concentrations of $MTSEA^+$ (typically 0.1, 0.25, 1, and 2.5 mM) (all in excess over the reactive sulfhydryls). The fraction of initial binding (Y) was fit to e^{-kct}, where k is the second-order rate constant, c is the concentration of $MTSEA^+$, and t is the time (120 s).

RESULTS

Effects of Cysteine Substitution on Antagonist Binding. In a background of the mutant C118S, which is relatively insensitive to the MTS reagents (*6*), we mutated to cysteine, one at a time, 22 consecutive residues, Ile377−His398, in M6. Each mutant receptor was transiently or stably expressed in HEK 293 cells, and the K_D and B_{MAX} characterizing the equilibrium binding of the radiolabeled antagonist, [^{3}H]-*N*-methylspiperone, were determined. At 18 positions, the K_D of the cysteine-substitution mutant was between 0.7 and 2.5 times the K_D of C118S; in P388C and F390C, the K_D's were 3.7 and 3.1 times the K_D of C118S, respectively (Table 1). For these 20 mutants, B_{MAX} ranged from 10 to 110% of that obtained with C118S (Table 1). For W386C and F389C, the affinity of [^{3}H]-*N*-methylspiperone was too low for accurate determination of the K_D and B_{MAX} from saturation experiments; for these mutants, the IC_{50}'s for unlabeled *N*-methylspiperone in competition with [^{3}H]-*N*-methylspiperone were 2−3 orders of magnitude greater than that for C118S (Table 1).

Table 1: Characteristics of [^{3}H]-*N*-Methylspiperone Binding to Cysteine-Substituted Dopamine D2 Receptor[a]

mutant	K_D (pM)	K_{MUT}/K_{C118S}	$B_{MAX\ (fmol/cm^2)}$	*n*
I377C	62 ± 14	0.8	176 ± 58	2
V378C	75 ± 14	0.9	250 ± 66	3
L379C	58 ± 10	0.7	147 ± 13	2
G380C	49 ± 2	0.6	226 ± 55	2
V381C	61 ± 5	0.8	293 ± 21	2
F382C	121 ± 31	1.5	97 ± 1	2
I383C	66 ± 13	0.8	136 ± 10	2
I384C	55 ± 13	0.7	265 ± 57	2
C385 (C118S)	79 ± 14	1.0	373 ± 31	5
W386C[b]	110 ± 30 nM	1600	ND	5
L387C	96 ± 2	1.2	283 ± 36	2
P388C	292 ± 59	3.7	34 ± 9	4
F389C[b]	6600 ± 650	82	ND	4
F390C	243 ± 11	3.1	149 ± 31	3
I391C	127 ± 17	1.6	272 ± 62	2
T392C	86 ± 11	1.1	152 ± 0	2
H393C	59 ± 12	0.7	244 ± 62	3
I394C	80 ± 10	1.0	250 ± 76	2
L395C	148 ± 49	1.9	351 ± 31	2
N396C	196 ± 27	2.5	365 ± 73	2
I397C	97 ± 12	1.2	178 ± 52	2
H398C	62 ± 23	0.8	411 ± 216	2

[a] Cells transfected with the appropriate receptor were assayed as described in Experimental Procedures. Data were fit to the binding isotherm by nonlinear regression. The means and SEM are shown for *n* independent experiments, each with duplicate determinations. B_{MAX} values are presented as femtomoles per square centimeter of plate area. [b] The values shown for W386C and F389C are IC_{50} values determined from the competition of [^{3}H]-*N*-methylspiperone by unlabeled *N*-methylspiperone. ND, not determined.

Table 2: Inhibitory Potency of (−)-Sulpiride on [^{3}H]-*N*-Methylspiperone Binding to Cysteine-Substituted Dopamine D2 Receptor[a]

mutant	apparent K_I (nM)	*n*	$K_{I(MUT)}/K_{I(C118S)}$
I377C	11 ± 2	2	1.6
V378C	3 ± 1	2	0.4
L379C	3 ± 0	2	0.5
G380C	4 ± 1	2	0.7
V381C	4 ± 1	2	0.6
F382C	54 ± 13	3	8.0
I383C	7 ± 1	2	1.0
I384C	3 ± 0	3	0.5
C385 (C118S)	7 ± 3	3	1.0
W386C	>10 μM	2	>1500
L387C	15 ± 1	2	2.2
P388C	65 ± 11	3	9.6
F389C	>10 μM	4	>1500
F390C	24 ± 11	2	3.5
I391C	15 ± 1	2	2.2
T392C	10 ± 3	2	1.4
H393C	54 ± 0	2	8.0
I394C	5 ± 1	2	0.8
L395C	8 ± 1	2	1.2
N396C	10 ± 7	2	1.4
I397C	8 ± 2	2	1.2
H398C	12 ± 5	2	1.8

[a] Cells transfected with the appropriate receptor were assayed with [^{3}H]-*N*-methylspiperone (150 pM) as described in Experimental Procedures in the presence of nine concentrations of (−)-sulpiride. The apparent K_I was determined by the method of Cheng and Prusoff (*41*) using the IC_{50} value obtained by fitting the data to a one-site competition model by nonlinear regression. The means and SEM are shown for *n* independent experiments, each with duplicate determinations.

The K_I of the antagonist sulpiride in competition with [^{3}H]-*N*-methylspiperone was determined in the 22 mutants (Table 2). At 16 positions, the K_I was between 0.4 and 2.2 times the K_I of C118S; in F382C, P388C, F390C, and H393C, the K_I was between 3.5 and 9.6 times the K_I of C118S. In W386C and F389C the IC_{50} was >10 mM, more than 1500-fold higher than the K_I of C118S.

Reactions of MTSEA$^+$ with the Mutants. When statistical significance was defined by Dunnett's post hoc test, 2.5 mM MTSEA$^+$ significantly inhibited [^{3}H]-*N*-methylspiperone binding to 10 of 22 cysteine-substitution mutants (Figure 1A). MTSEA$^+$ at 0.25 mM significantly blocked binding to 7 of these 10 mutants (Figure 1B). The magnitude of inhibition by 2.5 mM MTSEA$^+$ was small for the three mutants, I377C, V378C, and I397C, which were not significantly inhibited by 0.25 mM MTSEA$^+$; moreover, the statistical significance of the reaction with these three mutants depended on the choice of the post hoc test. Thus, we were not confident that these three substituted cysteines reacted with MTSEA$^+$. If, however, reaction of MTSEA$^+$ with a substituted cysteine produced no change or only a small change in binding, then our use of binding as an indirect measure of reaction might produce a false negative conclusion about the accessibility of the engineered cysteine. Indeed, we previously found that modification of Cys118 with MTSEA$^+$ affected the binding of the antagonist [^{3}H]YM-09151-2, a substituted benzamide, much more than it affected the binding of [^{3}H]-*N*-methylspiperone (*20*). Therefore, for all of the mutants which were negative at 0.25 mM MTSEA$^+$, we determined the effect of 2.5 mM MTSEA$^+$ on [^{3}H]YM-09151-2 binding (Figure 2). [^{3}H]YM-09151-2 binding to V378C, F382C, and I397C was significantly inhibited by 2.5 mM MTSEA$^+$, while the binding to I377C was not significantly inhibited.

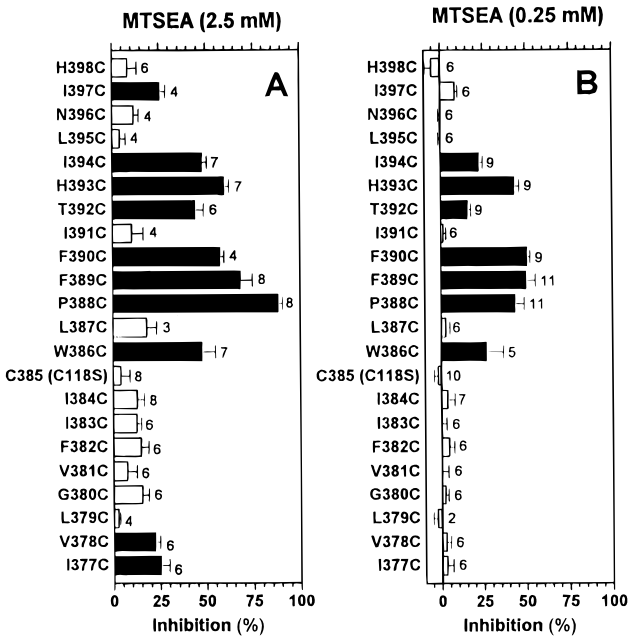

FIGURE 1: Inhibition of specific [^{3}H]-*N*-methylspiperone (200 pM) binding to intact cells transfected with wild-type or mutant D2 receptors resulting from a 2 min application of (A) 2.5 mM MTSEA$^+$ or (B) 0.25 mM MTSEA$^+$. The means and SEM are shown. The number of independent experiments for each mutant is shown next to the bars. Solid bars indicate mutants for which inhibition was significantly different ($p < 0.05$) from that of C385 (C118S) by one-way ANOVA.

To quantitate the susceptibility to MTSEA$^+$, we determined the second-order rate constants for the reaction with MTSEA$^+$ (Table 3).The most reactive cysteines were those substituted for Phe390 and His393. Cysteines substituted

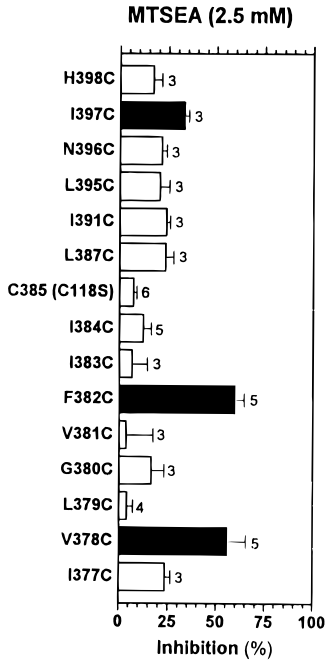

FIGURE 2: Inhibition of specific [^{3}H]YM-09151-2 (200 pM) binding to intact cells transfected with wild-type or mutant D2 receptors resulting from a 2 min application of 2.5 mM MTSEA$^+$. The means and SEM are shown. The number of independent experiments for each mutant is shown next to the bars. Solid bars indicate mutants for which inhibition was significantly different ($p < 0.05$) from that of C385 (C118S) by one-way ANOVA.

Table 3: Rates of Reaction of MTSEA$^+$ with Cysteine-Substituted Dopamine D2 Receptor[a]

mutant	k_{MTSEA} (M^{-1} s^{-1})	k_{MUT}/k_{WT}
V378C	5 ± 0	0.1
F382C	4 ± 1	0.1
W386C	ND	
P388C	13 ± 4	0.3
F389C	ND	
F390C	88 ± 10	1.7
T392C	4 ± 0	0.1
H393C	86 ± 18	1.7
I394C	15 ± 3	0.4
I397C	ND	

[a] The second-order rate constant (k) was determined as described in Experimental Procedures. We could not accurately determine rates for W386C and F389C because of the low affinity of binding and for I397C because of the small effect of 2.5 mM MTSEA$^+$. Rates for V378C and F382C were determined with [^{3}H]YM-09151-2 instead of [^{3}H]-*N*-methylspiperone. The means and SEM of two or three independent experiments, each performed with triplicate determinations, are shown. k_{MUT}/k_{WT} was obtained by dividing each k value by the k determined for the wild-type receptor in which Cys118 reacts (not C118S, which does not react and which is the background for all the other mutants).

for Pro388 and Ile394 were of intermediate reactivity with MTSEA$^+$. Cysteines substituted for Val378, Phe382, and Thr392 were least reactive. (We could not accurately determine rates for W386C and F389C because of the low affinity of binding and for I397C because of the small effect of 2.5 mM MTSEA$^+$.) The reversible antagonist sulpiride significantly retarded the reaction of MTSEA$^+$ with V378C, F382C, P388C, F390C, T392C, and I394C. (Protection could not reliably be determined with W386C, F389C, or I397C due to the low affinity of binding or the small effect of MTSEA$^+$.) The degree of protection varied from 40 to 100% (Figure 3). In contrast, sulpiride did not significantly slow the reaction of H393C with MTSEA$^+$.

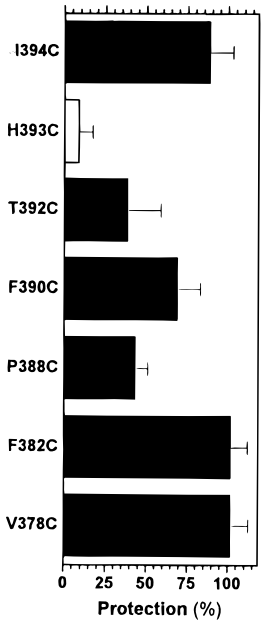

FIGURE 3: Sulpiride protection of cysteine-substitution mutants. Dissociated cells were incubated in buffer A for 20 min at room temperature in the presence or absence of (±)-sulpiride, and then MTSEA$^+$ was added, in the continued presence or absence of sulpiride, for 2 min at a concentration chosen to inhibit 50−75% of specific binding in the absence of sulpiride. Concentrations of MTSEA$^+$ were as follows: 2.5 mM V378C and F382C, 2 mM T392C, 1 mM P388C, 0.5 mM I394C, and 0.25 and 0.1 mM H393C and F390C, respectively. For most mutants, sulpiride was used at a concentration of 10 μM. To compensate for changes in the K_I, sulpiride concentrations were adjusted for several mutants as follows: 20 μM F390C, 50 μM F382C and P388C, and 100 μM H393C. Cells were washed by filtration though 96-well multiscreen plates containing GFB filters (Millipore). In the wash buffer, sodium was replaced by choline in order to facilitate removal of residual sulpiride. [^{3}H]-*N*-Methylspiperone binding ([^{3}H]YM-09151-2 binding for V378C and F382C) to the washed cells was performed in buffer A in the multiscreen plates in a final volume of 0.25 mL. The means and SEM of two to five independent experiments, each performed with triplicate determinations, are shown. Protection was calculated as 1 − [(inhibition in the presence of sulpiride)/(inhibition in the absence of sulpiride)]. Protection by sulpiride was significant ($p < 0.05$) by paired t-test for all of the mutants (filled bars) except H393C (unfilled bar).

Reactions with MTSET$^+$ and MTSES$^-$. All seven of the mutants most sensitive to MTSEA$^+$ (Figure 1B) were susceptible to reaction with 1 mM MTSET$^+$ (Figure 4A). At 10 mM, MTSES$^-$, the negatively charged derivative, significantly inhibited binding to five of the seven mutants that were susceptible to MTSET$^+$ and also to F382C for which inhibition by MTSET$^+$, despite being of comparable magnitude, did not reach statistical significance (Figure 4B).

DISCUSSION

Residues Forming the Water-Accessible Surface of the Binding-Site Crevice. We identify residues on the water-accessible surface of the D2 receptor by the ability of the MTS reagents to react with substituted cysteine residues. We assume that the MTS reagents will react much faster with water-accessible cysteine residues than with cysteines facing the protein interior or lipid because the reagents are highly polar. Furthermore, they react 10^9 times faster with ionized

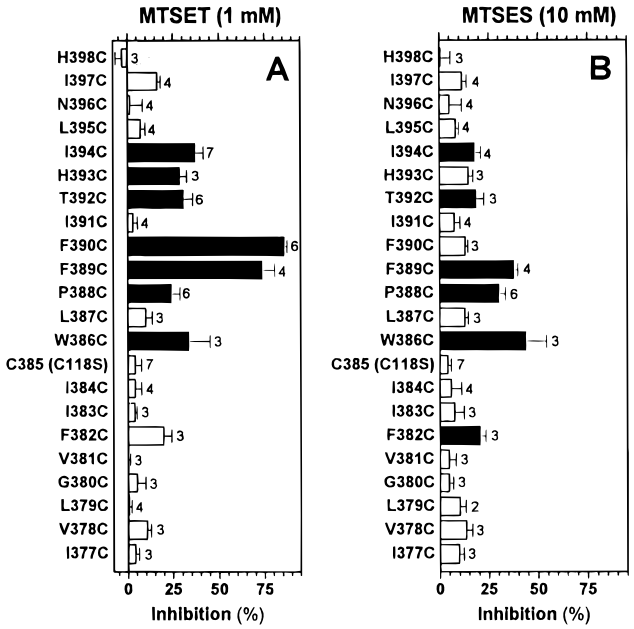

FIGURE 4: Inhibition of specific [^{3}H]-*N*-methylspiperone (200 pM) binding to intact cells transfected with wild-type or mutant D2 receptors resulting from a 2 min application of (A) 1 mM MTSET$^+$ or (B) 10 mM MTSES$^-$. On the basis of the relative rate constants for reaction with simple thiols in solution, namely 10:4:1 for MTSET$^+$, MTSEA$^+$, and MTSES$^-$ (*10*), we used equireactive concentrations of 1 mM MTSET$^+$ (A) and 2.5 mM MTSEA$^+$ (Figure 1A) and 10 mM MTSES$^-$ (B). The means and SEM are shown. The number of independent experiments for each mutant is shown next to the bars. Solid bars indicate mutants for which inhibition was significantly different ($p < 0.05$) from that of C385 (C118S) by one-way ANOVA.

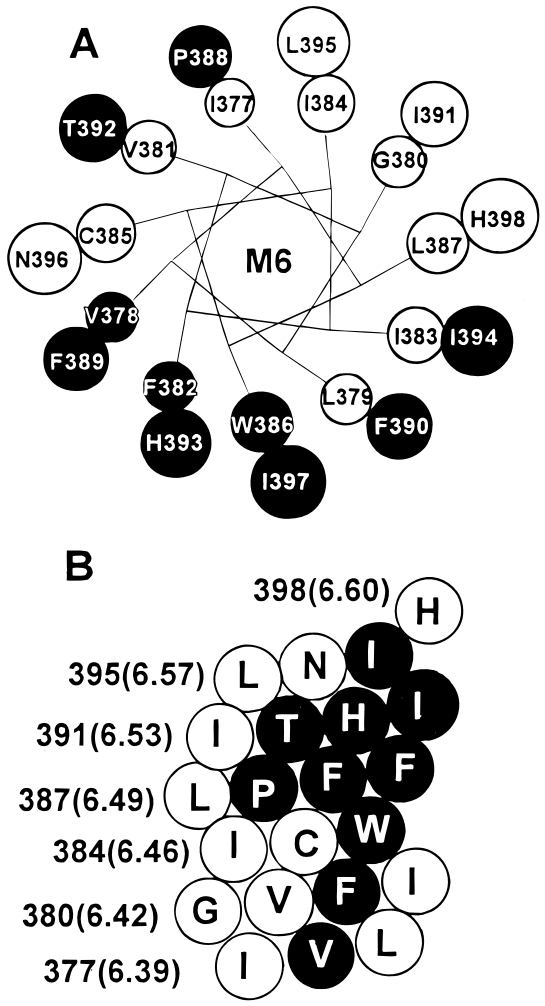

FIGURE 5: Helical net (A) and helical wheel (B) representations of the residues in and flanking the M6 segment of the dopamine D2 receptor, summarizing the effects of MTSEA$^+$ on [^{3}H]-*N*-methylspiperone and [^{3}H]YM-09151-2 binding. Reactive residues are filled, and open circles indicate that MTSEA$^+$ had no significant effect on binding. In panel A, increasing sizes of the circles indicate increasingly extracellular localization of the indicated residues.

thiolates than with un-ionized thiols (*21*), and only water-accessible cysteines are likely to ionize to a significant extent. We infer that the MTS reagents have reacted if the binding of ligand is irreversibly affected. Thus, we infer that 10 of the 22 residues tested are on the water-accessible surface of the D2 receptor. These residues are Val378$^{(6.40)}$, Phe382$^{(6.44)}$, Trp386$^{(6.48)}$, Pro388$^{(6.50)}$, Phe389$^{(6.51)}$, Phe390$^{(6.52)}$, Thr392$^{(6.54)}$, His393$^{(6.55)}$, Ile394$^{(6.56)}$, and Ile397$^{(6.59)}$ (Figure 1).

The residues that form the surface of the binding-site crevice are a subset of the water-accessible residues. We infer that water-accessible residues are in the binding-site crevice if the reaction of the MTS reagents is retarded by competitive antagonists or agonists. The competitive antagonist sulpiride protected all of the residues tested except H393C. We were unable to test for sulpiride protection with the mutants W386C and F389C because the binding affinity was too low and with the mutant I397C because the inhibition by MTSEA$^+$ was too small.

The extent of protection by sulpiride varied considerably among the mutants (Figure 3). Protection of a substituted cysteine is most simply explained by its proximity to the sulpiride binding site. Nevertheless, not every one of these residues need contact sulpiride. Sulpiride could protect residues deeper in the crevice by binding above them and blocking the passage of MTSEA$^+$ from the extracellular medium toward the cytoplasmic end of the crevice. We also cannot rule out indirect effects through propagated structural changes for the protection by sulpiride. The reason for the inability of sulpiride to protect H393C is not clear. Sulpiride's affinity was reduced nearly 10-fold in this mutant. A similar 10-fold reduction in the affinity of sulpiride was seen after mutation of this histidine to leucine (*22*). The effects of this mutation were highly specific; only the affinities of certain members of the substituted benzamide class of antagonists were altered. The decrease in affinity for sulpiride was hypothesized to result from the loss of a hydrogen bond between His393 and the 5-sulfonamide of sulpiride. Loss of this interaction may prevent bound sulpiride from protecting the substituted cysteine in H393C from reaction with MTSEA$^+$. In addition, if the increase in the K_I of sulpiride in H393C results primarily from an increase in the dissociation rate of the ligand, this may also decrease the ability of sulpiride to protect the engineered cysteine.

Reaction of a MTS reagent with an accessible cysteine can inhibit ligand binding through a number of mechanisms, including steric block, electrostatic repulsion, and/or an indirect structural effect on the binding site. Whatever the mechanism of irreversible inhibition by the MTS reagents, the effect itself, however, is evidence that the reaction had occurred. Moreover, that the effect is seen with any ligand is evidence that reaction had occurred. Reaction of MTSEA$^+$

with I378C and with F382C had a larger effect on the binding of [^{3}H]YM-09151-2 than on that of [^{3}H]-*N*-methylspiperone. This is similar to the greater effect of modification of Cys118 on the affinity of the substituted benzamides (*20*). If these compounds extend deeper in the binding-site crevice, then their binding might be more sensitive to the modification of these more cytoplasmic residues. Another possibility, however, is that the substituted benzamides may be more sensitive to an indirect structural perturbation of the binding site than is *N*-methylspiperone. Indeed, *N*-methylspiperone binding is insensitive to the presence or absence of sodium while the affinities of substituted benzamides are sodium-dependent (*23*, *24*). Thus, compounds such as YM-09151-2 and sulpiride can differentiate conformational states of the binding site which *N*-methylspiperone cannot.

Secondary Structure of M6. The pattern of the residues which are accessible to the MTS reagents is consistent with M6 being α-helical, with a wide exposure for two helical turns near the binding site and a narrower stripe continuing toward the cytoplasm (Figure 5). A possible explanation for the broadening of exposure, which begins at Pro388, is the presence of a proline kink (*25*) at this position. Such a kink could bend the extracellular portion of M6 toward the binding-site crevice where a wide arc would be exposed to $MTSEA^+$ (Figure 6). In contrast, the portion of M6 more cytoplasmic than the proline kink is either tightly packed against neighboring membrane-spanning segments or exposed to lipid, resulting in an accessibility to $MTSEA^+$ which is restricted to a narrow stripe in this region.

Interestingly, highly conserved Pro residues are found in M2, M5, M6, and M7 of GPCRs and may play a crucial structural and functional role (*26*−*29*). In M7 of the D2 receptor, the pattern of accessibility of the cysteine-substitution mutants was consistent with M7 being a kinked α-helix, but in this case, a significant face twist at the kink was required to fit the experimental data (*9*). In M6, the pattern of accessibility is straight, and thus, a simple bend and/or conformational flexibility at the Pro kink is sufficient to explain the data (Figure 6).

A possible mechanism of receptor activation utilizing flexibility about the proline kink in M6 has been proposed (*15*, *16*). Movement of M6 has been demonstrated in the homologous β2 adrenergic receptor by monitoring the position of Cys285$^{(6.47)}$, the residue which aligns with D2 receptor Cys385$^{(6.47)}$. We have demonstrated that, while Cys285 is not accessible in the binding-site crevice of the wild-type β2 receptor, this residue becomes accessible in the binding-site crevice of a constitutively activated β2 receptor (*13*). A rotation or translational movement of M6 would be sufficient to bring this cysteine to the margin of the binding-site crevice. Indeed, such a rotation and/or translational movement of M6 was found to be necessary for the activation of rhodopsin (*12*, *30*). Movement about the postulated proline kink could produce such a rotation or tilting without requiring a movement of the entire membrane-spanning segment (see Figure 4c in ref *14*).

According to the model, Asn396$^{(6.58)}$, at the extracellular end of M6, is located within a continuous surface patch on M6 that is accessible to $MTSEA^+$. However, none of the MTS reagents had a significant effect on antagonist binding to N396C. Thus, the engineered cysteine at this position may be inaccessible to the MTS reagents and, therefore, not on the water-accessible surface of the protein. It is also possible, however, that local steric factors may make a water-accessible residue inaccessible to the MTS reagents. In addition, in rare cases, a residue forming the surface of the binding-site crevice could be covalently modified by the addition of the charged SCH_2CH_2X without interfering with binding (*20*).

Comparison of Reactions with $MTSEA^+$ and $MTSET^+$. When adjusted for the rate constants for their reactions with simple thiols in solution (*10*), the reaction of $MTSEA^+$ with cysteines in the binding-site crevice is accelerated approximately 10-fold relative to that of $MTSET^+$ (Figures 1 and 4A). $MTSEA^+$ is smaller than $MTSET^+$, and its access to substituted cysteines may be less sterically hindered. Moreover, $MTSEA^+$, like dopamine, contains an ethylammonium group, and it could be the affinity of this group for the dopamine-binding site that accelerates the reaction of $MTSEA^+$ relative to that of $MTSET^+$. This pattern is broken, however, by F389C and F390C, which are nearly equireactive with $MTSEA^+$ and $MTSET^+$. Thus, at these positions, the reaction of $MTSET^+$ is accelerated approximately 10-fold relative to that of $MTSEA^+$. We observed a similar effect with T412C in M7 (*9*), and we noted that the specific increase may be the result of an interaction of the aromatic side chains of Trp413$^{(7.40)}$ and Tyr416$^{(7.43)}$ with the hydrophobic quaternary ammonium group of $MTSET^+$ (*31*) which would favor the reaction with $MTSET^+$ at T412C. The cluster of aromatic residues in M6, Phe382, Trp386, Phe389, Phe390, and His393 (Figure 7A,B), could have a similar effect. In particular, favorable interactions of the $MTSET^+$ cation with Trp386 and other nearby aromatic side chains are likely to be responsible for the increase in reactivity seen at F389C and F390C (Figure 7C,D). Aromatic residues from other membrane-spanning segments may also contribute to this enhanced reactivity; in particular, Tyr416$^{(7.43)}$ in M7 and Phe198$^{(5.47)}$ in M5 are accessible in the binding-site crevice (*8*, *9*), and both of these residues are likely to be adjacent to this aromatic-rich region of M6.

The Binding Site and the Aromatic Cluster. The four accessible aromatic residues in the cluster (Figure 7A,B) are completely conserved within related neurotransmitter GPCRs, and some of these residues have been show to be important for ligand binding and/or receptor activation (*32*, *33*). Molecular modeling simulations have suggested that the conformations of the side chains of these aromatic residues are interdependent and that ligand binding may induce coordinated movements of these residues, resulting in a rotational/translational movement about the proline kink.[2] Ligand−receptor interactions that can be supported by such an "aromatic cluster" have been suggested from structure−activity data for dopamine agonists acting on the D2 receptor (*34*). Suggested requirements for potency included an electrostatic interaction between the protonated amine and a negative subsite which has been established to be Asp114 in M3 (*7*, *35*, *36*), a hydrogen bonding group or groups which interact with a serine or serines in M5 (*36*−*38*), and an aromatic ring which interacts with a hydrophobic site. This hydrophobic site is likely to be the aromatic cluster in M6 which extends to the adjacent M5 where it includes

[2] J. A. Ballesteros and H. Weinstein, to be published.

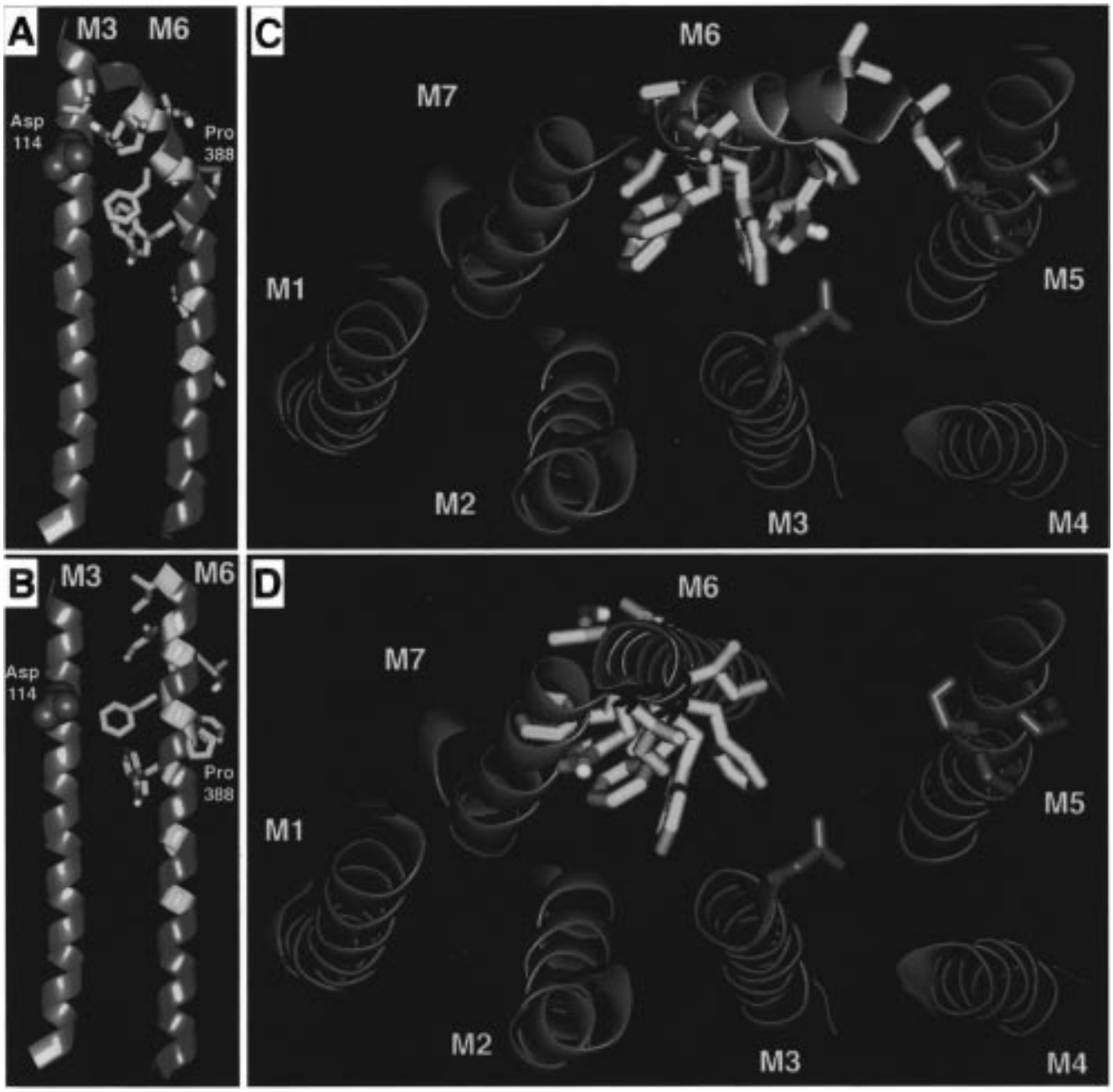

FIGURE 6: Molecular models of M6 illustrating how the bending induced by a proline kink could explain the extracellular broadening in the pattern of residues accessible in the binding-site crevice. A side view of M6 and M3 (A) shows that the bend at Pro388 brings the residues accessible to $MTSEA^+$ (yellow) toward the binding-site crevice indicated by Asp114 (purple) in M3, compared to panel B which is the pattern in an ideal α-helix. Note that the cytoplasmic portion of M6 is oriented similarly in all panels; these models differ only in the extracellular portions. The relative positioning of M6 and M3 follows the experimentally derived data on M3−M6 proximity in rhodopsin (*12*). Panels C and D show an extracellular view of the observed $MTSEA^+$ accessibility pattern in M6 in the context of the entire bundle of seven transmembrane segments arranged following the rhodopsin projection map (*42*), for panel C a proline-kinked M6 and for panel D an ideal α-helix. The position of the binding site is indicated by Asp114 in M3 and Ser203, Ser204, and Ser207 in M5 (all in purple) (*11*). Note the proximity of the accessible residues in M6 (yellow) to the binding-site crevice in the kinked helix (C) but not in the ideal helix (D). Furthermore, several residues accessible to the polar MTS reagents, such as Pro388 and Thr392, would be facing the lipid membrane in an ideal α-helix (D).

Phe198$^{(5.47)}$ and to the adjacent M7 where it includes Tyr416$^{(7.43)}$, both of which are also accessible in the binding-site crevice (*8*, *9*).

The role of some of these aromatic residues has been examined previously in the D2 receptor by mutation to alanine (*32*). In agreement with these previous results, we found F389C to bind both *N*-methylspiperone and sulpiride with greatly reduced affinity. Surprisingly, F390C had only an about 4-fold decreased affinity for *N*-methylspiperone, while F390A was reported to have undetectable binding (*32*). Thus, Cys is a much better tolerated substitution for Phe390 than is Ala. The Cys substituted for Phe390 may interact directly with ligand and/or stabilize the structure of the receptor by interacting with another residue. In known protein structures, about 50% of sulfur atoms from cysteine and methionine residues are in contact with an aromatic ring (*39*), and in model systems, these interactions at the *i* to (*i*-4) position can contribute up to 2 kcal/mol to α-helical

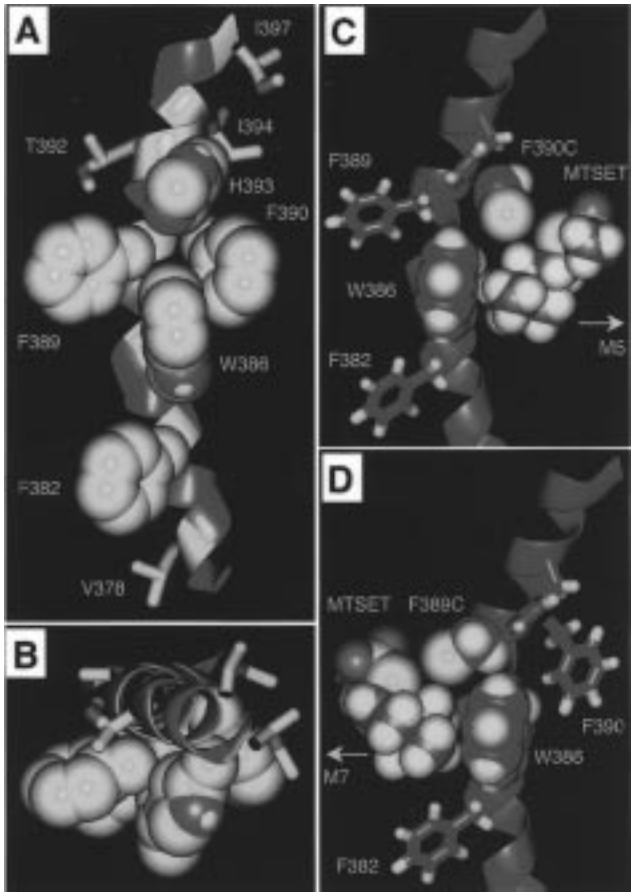

FIGURE 7: Molecular model showing the aromatic cluster in M6. Residues in M6 accessible to $MTSEA^+$ are shown in yellow in (A) a front view and (B) a top view from the extracellular side. Note the presence of a cluster of aromatic residues encompassing Phe382, Trp386, Phe389, Phe390, and His393, shown in van der Waals representations. This aromatic cluster could be responsible for the faster rates of reaction with $MTSET^+$, relative to $MTSEA^+$, with F389C and F390C, due to the attractive interactions of the hydrophobic quaternary ammonium group of $MTSET^+$ with the aromatic side chains, and in particular with Trp386 (panels C and D). Note that the interaction of $MTSET^+$ with Trp386 could be complemented by interactions with other aromatic side chains from neighboring helices, which according to the projection map in Figure 6 would be (C) M5 for F390C and (D) M7 for F389C (see the text). The proposed interaction of $MTSET^+$ with Trp386 can support an orientation of the methanethiosulfonate moiety relative to the substituted Cys at residues Phe389 (C) or Phe390 (D) that accommodates the stereochemical requirements of a nucleophilic reaction (SN2) between the substituted Cys and $MTSET^+$, thus contributing to the enhanced reaction rates.

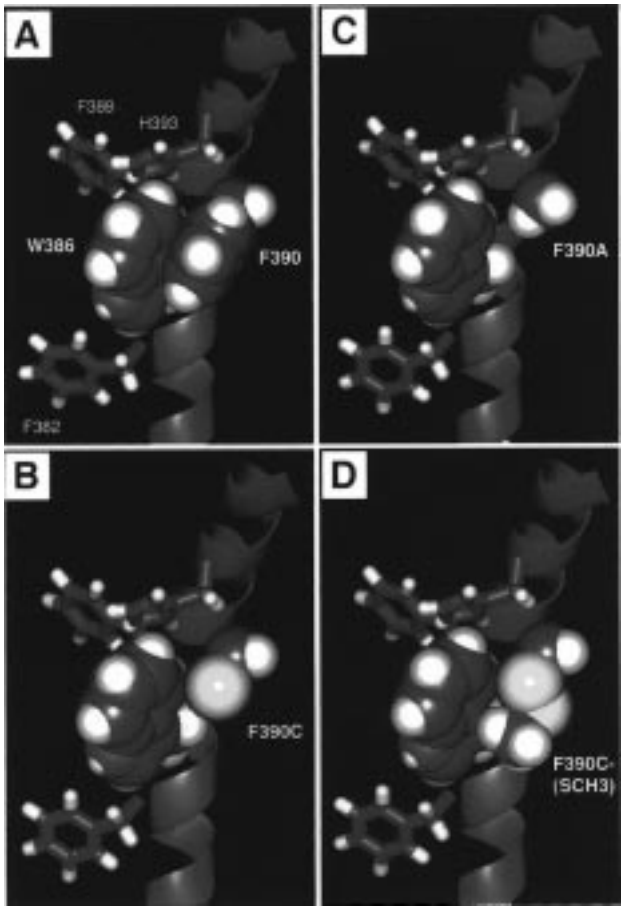

FIGURE 8: Interaction between Phe390 and Trp386 illustrated by van der Waals representations. Panel A shows the interaction of wild-type Phe390 and Trp386. In panel B, the F390C mutant, the cysteine sulfhydryl can partially replace the stabilizing effect of the wild-type aromatic−aromatic interaction between Phe390 and Trp386 with the known sulfur−aromatic interaction (*39*). F390C has only an about 4-fold decreased affinity for *N*-methylspiperone (see Table 1). In panel C, the mutant F390A, which does not bind *N*-methylspiperone (*33*), is depicted in the same geometry, indicating that it cannot support this type of interaction. In panel D, the side chain which results from the reaction of F390C with MMTS (which adds an SCH_3 group to the cysteine sulfhydryl) increases the compensating effect of the sulfur−aromatic interaction. MMTS reaction increases the affinity of F390C for *N*-methylspiperone 4-fold and restores the wild-type affinity (see the text).

stability (*40*). Thus, at position 390, the sulfur of cysteine (Figure 8B), but not the methyl group of the alanine (Figure 8C), may stabilize the aromatic cluster as illustrated in Figure 8 for the interaction with the adjacent aromatic ring of Trp386 at the (*i*-4) position.

We speculated that if the sulfur were critical to such an interaction then substitution at position 390 with Met, which is also closer in size to the endogenous Phe, might be even better tolerated than substitution with Cys. To test this hypothesis, we reacted with F390C the methylmethanethiosulfonate (MMTS) reagent, which adds the methionine-like SCH_3 side chain to the cysteine sulfhydryl. As predicted, reaction with MMTS with F390C (but not with W386C, F389C, or F382C) significantly potentiated *N*-methylspiperone binding (data not shown). Saturation analysis revealed that this potentiation resulted from a 4-fold increase in the affinity of the MMTS-modified receptor (data not shown) and is consistent with a more favorable interaction of the new methionine-like side chain with Trp386 at the (*i*-4) position as shown in the structural comparisons depicted in Figure 8. The methionine-like side chain may be a better substitute of Phe in the interaction with the aromatic moiety of bound ligand as well. This illustrates the potential utility of the MMTS reagent in probing the interactions contributed by aromatic microdomains to receptor stability and ligand binding.

ACKNOWLEDGMENT

We thank Drs. Olivier Civelli, Brian Kobilka, and Steve Rees for the human D2 receptor cDNA, the epitope-tagged β2 adrenergic receptor cDNA, and the pcin4 vector, respectively. We thank Thomas Livelli for the HEK 293 and the 293-TSA cells and for valuable advice. We thank Myles

Akabas and Arthur Karlin for valuable discussion and for comments on the manuscript.

REFERENCES

1. Civelli, O., Bunzow, J. R., Grandy, D. K., Zhou, Q. Y., and Van Tol, H. H. (1991) *Eur. J. Pharmacol. 207*, 277−286.
2. Strader, C. D., Fong, T. M., Tota, M. R., Underwood, D., and Dixon, R. A. (1994) *Annu. Rev. Biochem. 63*, 101−132.
3. Oprian, D. D. (1992) *J. Bioenerg. Biomembr. 24*, 211−217.
4. Akabas, M. H., Kaufmann, C., Archdeacon, P., and Karlin, A. (1994) *Neuron 13*, 919−927.
5. Akabas, M. H., Stauffer, D. A., Xu, M., and Karlin, A. (1992) *Science 258*, 307−310.
6. Javitch, J. A., Li, X., Kaback, J., and Karlin, A. (1994) *Proc. Natl. Acad. Sci. U.S.A. 91*, 10355−10359.
7. Javitch, J. A., Fu, D., Chen, J., and Karlin, A. (1995) *Neuron 14*, 825−831.
8. Javitch, J. A., Fu, D., and Chen, J. (1995) *Biochemistry 34*, 16433−16439.
9. Fu, D., Ballesteros, J. A., Weinstein, H., Chen, J., and Javitch, J. A. (1996) *Biochemistry 35*, 11278−11285.
10. Stauffer, D. A., and Karlin, A. (1994) *Biochemistry 33*, 6840−6849.
11. van Rhee, A. M., and Jacobson, K. A. (1996) *Drug Dev. Res. 37*, 1−38.
12. Farrens, D. L., Altenbach, C., Yang, K., Hubbell, W. L., and Khorana, H. G. (1996) *Science 274*, 768−770.
13. Javitch, J. A., Fu, D., Liapakis, G., and Chen, J. (1997) *J. Biol. Chem. 272*, 18546−18549.
14. Gether, U., Lin, S., Ghanouni, P., Ballesteros, J. A., Weinstein, H., and Kobilka, B. K. (1997) *EMBO J. 16*, 6737−6747.
15. Zhang, D., and Weinstein, H. (1993) *J. Med. Chem. 36*, 934−938.
16. Luo, X., Zhang, D., and Weinstein, H. (1994) *Protein Eng. 7*, 1441−1448.
17. Ballesteros, J. A., and Weinstein, H. (1995) *Methods Neurosci. 25*, 366−428.
18. Kobilka, B. K. (1995) *Anal. Biochem. 231*, 269−271.
19. Rees, S., Coote, J., Stables, J., Goodson, S., Harris, S., and Lee, M. G. (1996) *BioTechniques 20*, 102−110.
20. Javitch, J. A., Fu, D., and Chen, J. (1996) *Mol. Pharmacol. 49*, 692−698.
21. Roberts, D. D., Lewis, S. D., Ballou, D. P., Olson, S. T., and Shafer, J. A. (1986) *Biochemistry 25*, 5595−5601.
22. Woodward, R., Daniell, S. J., Strange, P. G., and Naylor, L. H. (1994) *J. Neurochem. 62*, 1664−1669.
23. Freedman, S. B., Poat, J. A., and Woodruff, G. N. (1982) *J. Neurochem. 38*, 1459−1465.
24. Niznik, H. B., Grigoriadis, D. E., Pri-Bar, I., Buchman, O., and Seeman, P. (1985) *Naunyn-Schmiedebergs Arch. Pharmacol. 329*, 333−343.
25. Barlow, D. J., and Thornton, J. M. (1988) *J. Mol. Biol. 201*, 601−619.
26. Ballesteros, J. A., and Weinstein, H. (1992) *Biophys. J. 62*, 107−109.
27. Sansom, M. S. (1992) *Protein Eng. 5*, 53−60.
28. Williams, K. A., and Deber, C. M. (1991) *Biochemistry 30*, 8919−8923.
29. Woolfson, D. N., Mortishire, S. R. J., and Williams, D. H. (1991) *Biochem. Biophys. Res. Commun. 175*, 733−737.
30. Sheikh, S. P., Zvyaga, T. A., Lichtarge, O., Sakmar, T. P., and Bourne, H. R. (1996) *Nature 383*, 347−350.
31. Dougherty, D. A. (1996) *Science 271*, 163−168.
32. Cho, W., Taylor, L. P., Mansour, A., and Akil, H. (1995) *J. Neurochem. 65*, 2105−2115.
33. Roth, B. L., Shomam, M., Choudhary, M. S., and Khan, N. (1997) *Mol. Pharmacol. 52*, 259−266.
34. Seeman, P. (1980) *Pharmacol. Rev. 32*, 229−313.
35. Strader, C. D., Sigal, I. S., Candelore, M. R., Rands, E., Hill, W. S., and Dixon, R. A. (1988) *J. Biol. Chem. 263*, 10267−10271.
36. Mansour, A., Meng, F., Meador, W. J. H., Taylor, L. P., Civelli, O., and Akil, H. (1992) *Eur. J. Pharmacol. 227*, 205−214.
37. Strader, C. D., Sigal, I. S., and Dixon, R. A. (1989) *Trends Pharmacol. Sci. 10* (Suppl.), 26−30.
38. Cox, B. A., Henningsen, R. A., Spanoyannis, A., Neve, R. L., and Neve, K. A. (1992) *J. Neurochem. 59*, 627−635.
39. Reid, K. S. C., Lindley, P. F., and Thornton, J. M. (1985) *FEBS Lett. 190*, 209−213.
40. Viguera, A. R., and Serrano, L. (1995) *Biochemistry 34*, 8771−8779.
41. Cheng, Y., and Prusoff, W. H. (1973) *Biochem. Pharmacol. 22*, 3099−3108.
42. Schertler, G. F. X., and Hargrave, P. A. (1995) *Proc. Natl. Acad. Sci. U.S.A. 92*, 11578−11582.

BI972241Y